THE JOURNAL OF BIOLOGICAL CHEMISTRY VOL. 289, NO. 16, pp. 11488–11496, April 18, 2014

Transient Covalent Interactions of Newly Synthesized Thyroglobulin with Oxidoreductases of the Endoplasmic Reticulum*

Received for publication, September 27, 2013, and in revised form, February 18, 2014 Published, JBC Papers in Press, March 5, 2014, DOI 10.1074/jbc.M113.520767

Bruno Di Jeso[‡1], Yoshiaki Morishita[§], Antonella S. Treglia[‡], Dario D. Lofrumento[¶], Giuseppe Nicolardi[¶], Francesco Beguinot[‖], Aaron P. Kellogg[§], and Peter Arvan[§2]

From the [‡]Laboratorio di Patologia Generale, Dipartimento di Scienze e Tecnologie Biologiche ed Ambientali, Università del Salento, 73100 Lecce, Italy, the [§]Division of Metabolism, Endocrinology and Diabetes, University of Michigan Medical School, Ann Arbor, Michigan 48105, [¶]Laboratorio di Anatomia Umana, Dipartimento di Scienze e Tecnologie Biologiche ed Ambientali, Universita' del Salento, 73100 Lecce, Italy, and [‖]Dipartimento di Scienze Mediche Traslazionali e Istituto di Endocrinologia ed Oncologia Sperimentale, Centro Nazionale delle Ricerche, Università Federico II, 80131 Napoli, Italy

Background: Secretory proteins acquire their native three-dimensional conformation through repeated brief interactions with ER chaperones and oxidoreductases.
Results: We have captured and defined previously unidentified disulfide adducts of newly synthesized thyroglobulin with ERp72 and CaBP1/P5.
Conclusion: Multiple oxidoreductases simultaneously engage thyroglobulin during its early folding in the ER.
Significance: Distinct chaperone/oxidoreductase partners coordinately engage this multi-domain secretory protein to promote its advancement to the native state.

Newly synthesized thyroglobulin (Tg), the thyroid prohormone, forms detectable high molecular weight mixed disulfide adducts: until now, only Tg "adduct B" was identified as primarily engaging the endoplasmic reticulum oxidoreductases ERp57 and protein disulfide isomerase. Here, we demonstrate that the faster migrating Tg adduct C primarily engages the CaBP1/P5 oxidoreductase, whereas the slower migrating Tg adduct A primarily engages ERp72. Upon siRNA-mediated knockdown of CaBP1/P5 or ERp72, adducts C or A, respectively, are decreased. Within the three Tg adduct bands that do not exhibit a precursor-product relationship, Tg exhibits distinct oxidation patterns. We present evidence suggesting that disulfide maturation occurs within Tg monomers engaged in each of the adduct bands. Moreover, the same Tg substrate molecules can form simultaneous mixed disulfides with both CaBP1/P5 and protein disulfide isomerase, although these are generally viewed as components of distinct oxidoreductase-chaperone protein complexes. Such substrate-oxidoreductase combinations offer Tg the potential for simultaneous oxidative maturation along different parallel tracks leading to the native state.

During and following translocation across the membrane of the endoplasmic reticulum (ER),[3] secretory proteins acquire much of their native conformation before export to the Golgi complex. Protein folding is a complex task facilitated and monitored by ER folding enzymes and molecular chaperones (1, 2). For many secretory proteins, acquiring a three-dimensional globular structure is linked to formation and isomerization of disulfide bonds (3). These covalent interactions are catalyzed by a group of ER oxidoreductases: resident proteins that belong to the protein disulfide isomerase (PDI) family comprising >20 members (4–7).

It is poorly understood why the ER needs so many simultaneously expressed ER oxidoreductases. One possibility is that each oxidoreductase exhibits enzymatic selectivity for the formation of a specific subset of disulfide bonds, or is committed to catalyze a specific type of reaction (4–7). Alternatively, the oxidoreductases may simply serve redundant function(s). The best characterized ER oxidoreductases are PDI and ERp57. PDI oxidase and isomerase activities have been demonstrated both *in vitro* (8) and *in vivo* (9, 10). ERp57 acts on substrates in conjunction with their interaction with ER lectin-chaperones calnexin (CNX) and calreticulin (CRT) (11–14) but occasionally may act directly on substrates independently of CNX/CRT (15, 16). CaBP1/P5 and ERp72 are less well understood. Earlier studies reported that P5 and ERp72 are found in a large multienzyme complex that also includes PDI and BiP (17), but subsequent studies have indicated that whereas ERp72 and CaBP1 are associated with BiP (18), PDI is recovered in a dis-

* This work was supported by a grant of "Fondazione Cassa di Risparmio di Puglia" (to B. D. J.) and National Institutes of Health Grant R01 DK40344 (to P. A.).

[1] To whom correspondence may be addressed: Laboratorio di Patologia Generale, Dipartimento di Scienze e Tecnologie Biologiche ed Ambientali, Facoltà di Scienze MFN, Università del Salento, Centro Ecotekne, 73100 Lecce, Italy. Tel.: 39-0832-298-912; Fax: 39-0832-298-626; E-mail: bruno.dijeso@unisalento.it.

[2] To whom correspondence may be addressed: Div. of Metabolism, Endocrinology, and Diabetes, University of Michigan, 5112 Brehm Ctr., 1000 Wall St., Ann Arbor, MI 48105-51714. Tel.: 734-936-5505; Fax: 734-936-6684; E-mail: parvan@umich.edu.

[3] The abbreviations used are: ER, endoplasmic reticulum; Tg, thyroglobulin; PDI, protein disulphide isomerase; CNX, calnexin; CRT, calreticulin; ERp72, endoplasmic reticulum protein 72; ERp57, endoplasmic reticulum protein 57; CaBP1, calcium binding protein 1; BiP, binding protein; GRP94, glucose responsive protein 94; NEM, *N*-ethylmaleimide; DSP, dithiobis(succinimidylpropionate); ChEL, cholinesterase-like.

tinct complex (19), indicating selective chaperone/oxidoreductase partnerships.

Native thyroglobulin (Tg), the precursor protein for thyroid hormone synthesis, is a homodimeric secretory glycoprotein of 660 kDa (20) with up to 60 intramolecular disulfide bonds (21). Tg has several distinct regions bearing multiple independent folding units (22, 23). The N-terminal 1196 amino acids of Tg contain 10 repeating units (type 1 repeats) of ~60 amino acids with six cysteines engaged in internal Cys^1-Cys^2, Cys^3-Cys^4 and Cys^5-Cys^6 disulfide bonds, a pattern identical to that of other Tg protein family relatives (24, 25). The mid-portion of Tg contains two other types of cysteine-rich domains (type 2 and 3 repeats); it is highly likely that these repeats also use primarily internal disulfide bonds within their respective domain structures, as this mid-portion of the Tg molecule can itself function as a successful secretory protein (23). Finally, the C-terminal cholinesterase-like (ChEL) domain of Tg can also function as a successful secretory protein in its own right (26) with all cysteine residues engaged in internal disulfide bonds (27). However, some of the final disulfide loops to form in Tg may potentially involve long stretches of intervening primary sequence, including a few disulfide pairings located within Tg region I (28). The overall disulfide maturation of newly synthesized Tg is quite slow: completion of its oxidative folding requires ~60 to 90 min (22) and the half-time to medial Golgi arrival is 90–120 min (21).

The slow maturation makes Tg a good substrate in which to study chaperone/oxidoreductase-assisted folding. Multiple ER chaperone proteins, including CRT/CNX (22) and BiP (29) have been implicated in Tg folding. Moreover, we have observed transient mixed disulfide-linked adducts with endogenous oxidoreductases ERp57 and PDI (30) and others that are the focus of the present investigation, which may signify intermediates in the Tg folding pathway. Herein, we have definitively identified distinct mixed disulfide-linked adducts between newly synthesized Tg and ER oxidoreductases ERp72 and CaBP1/P5 and provide evidence to suggest that Tg oxidative maturation occurs within these distinct adduct bands, facilitating multidomain disulfide maturation within Tg monomers.

EXPERIMENTAL PROCEDURES

Materials—Coon's modified Ham's F-12 medium was from Sigma. Protein A-Sepharose was from Calbiochem. [^{35}S]cysteine and [^{35}S]methionine Promix and pure [^{35}S]methionine were from Amersham Biosciences. All other chemicals were from Sigma. Polyclonal rabbit anti-Tg antibodies were raised against rat Tg as described previously, using follicular mature rat Tg as antigen (31). Monoclonal anti-HA was from Covance. Polyclonal anti-CRT, anti-GRP94, anti-BiP, anti-PDI, anti-CNX, and anti-ERp72 antibodies were from Affinity Bioreagents and Stressgen and as described previously (30). Rabbit anti-ERp57 antibodies were a gift of Dr. T. Wileman (University of East Anglia); rabbit anti-CaBP1 antibodies were a gift of Dr. Phuc Nguyen Van (Georg-August University, Goettingen, Germany).

Cell Culture and Biological Reagents—PC Cl3 cells are a cloned line of differentiated thyroid follicular epithelial cells that were maintained as described previously (31). 293T cells were cultured in DMEM with 10% fetal bovine serum and penicillin (100 units/ml) and streptomycin (100 μg/ml).

RNA Interference—Selected predesigned siRNAs (60 nM; Ambion) specific for ERp72, or P5, or a negative nontargeting control, were mixed with 6 μl of RNAimax Lipofectamine (Invitrogen) in a final volume of 0.4 ml of Opti-MEM medium in six-well plates. To each well, 2.5×10^5 PC Cl3 cells in 1.6 ml of Opti-MEM were added and, after 4 h at 37 °C, the medium was supplemented with 1 ml of Coon's modified Ham's F-12 medium, calf serum to a final concentration of 5%, and the six hormones mixture to a final 1× concentration. After 3 days, the cells were either directly lysed for Western blot or metabolically labeled with ^{35}S-labeled amino acids for Tg immunoprecipitation as outlined below.

Metabolic Labeling and Immunoprecipitation—Metabolic labeling and immunoprecipitation were carried out as reported previously (30, 32). Briefly, for pulse-labeling, PC Cl3 cells were incubated for 30 min in methionine-free, cysteine-free medium, labeled for 15 min (unless otherwise indicated) at 37 °C in the same medium containing 50 μCi/ml [^{35}S]cysteine and [^{35}S]methionine labeling mix and either lysed without chase or chased in complete medium with an excess of cold methionine and cysteine. All subsequent manipulations were performed at 4 °C. For DTT washout experiments, PC Cl3 cells were treated with different concentrations of DTT and labeled as outlined above in the presence of DTT at the concentrations indicated. Cells were extensively washed with cold phosphate-buffered saline (PBS) to remove DTT before chase. At the end of chase, labeled cells were washed with cold PBS containing 20 mM *N*-ethylmaleimide (NEM) to alkylate free sulfhydryls. For long term labeling to approach steady state, cells were labeled at 500 μCi/ml pure [^{35}S]methionine for 48 h in complete medium (containing cysteine, methionine, and serum).

Cells were lysed in 1 ml of lysis buffer (150 mM NaCl, 0.5% Triton X-100, 25 mM Tris (pH 7.4), and complete protease inhibitor mixture (Roche Applied Science) plus 20 mM NEM. Nuclei and cell debris were removed by centrifugation at $10{,}000 \times g$ for 10 min at 4 °C. Lysates were incubated for 1 h at 4 °C with the respective antibodies and tumbled with protein A-Sepharose for 3 h. The beads were washed three times with lysis buffer and boiled in SDS sample buffer (4% SDS, 0.2% bromphenol blue, 20% glycerol, 100 mM Tris-HCl (pH 6.8)) with or without 20 mM dithiothreitol, and the supernatant was subjected to SDS-PAGE and autoradiography.

For immunoprecipitation in denaturing conditions, cells were labeled, washed, and lysed as described above. One-half of the lysate was immunoprecipitated as described above, and the other half was brought to 5% SDS and boiled for 5 min. The latter samples were then diluted 10-fold with 1% Triton X-100 in 150 mM NaCl, 25 mM Tris (pH 7.4). Immunoprecipitates of denatured samples were washed three times with 0.05% Triton X-100, 0.1% SDS, 0.3 M NaCl, 10 mM Tris (pH 8.6). For BiP immunoprecipitation, labeled cells were washed with cold PBS containing 20 mM NEM and then three times with PBS alone and lysed in 1 ml of lysis buffer plus 20 units/ml apyrase (to enzymatically deplete ATP). After 60 min, cells were processed as described above. Chemical cross-linking *in situ* was performed as reported previously (33) with minor modifications.

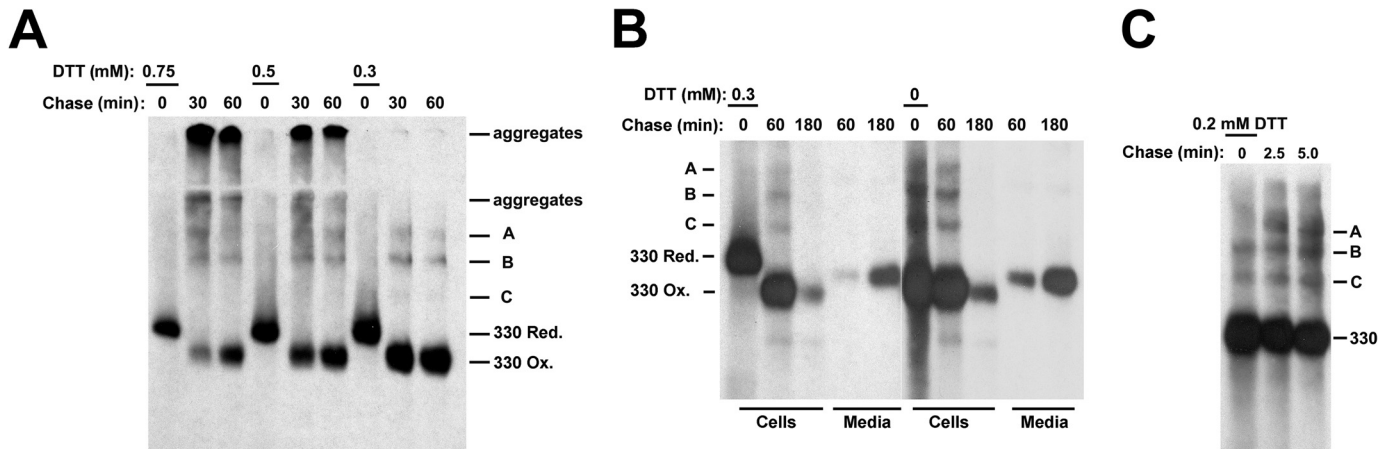

FIGURE 1. **Intermolecular disulfide-linked Tg adducts differ in their oxidation state.** PC Cl3 cells were pulse-labeled with ^{35}S-labeled amino acids in the presence of DTT at the concentrations shown. Cells were washed free of DTT and chased for the indicated times in the absence of reducing agent as outlined under "Experimental Procedures." *A*, cell lysates were immunoprecipitated with anti-Tg antibodies. Immunoprecipitates were resolved by SDS-PAGE under nonreducing conditions. The positions of reduced 330-kDa Tg at the end of the DTT treatment (*330 Red.*) and upon oxidation after DTT washout (*330-Ox.*) of intermolecular disulfide-linked adducts (A, B, and C) and Tg aggregates, are indicated on the panel. The gels were intentionally overexposed in order to optimally visualize the presence of bands A, B, and C. *B*, PC Cl3 cells were pulse-labeled with ^{35}S-labeled amino acids in the presence or absence of 0.3 mM DTT. Cells were washed free of DTT and chased for the indicated times in the absence of reducing agent as described under "Experimental Procedures." Cell lysates and culture media were immunoprecipitated with anti-Tg antibodies. Immunoprecipitates were resolved by SDS-PAGE under nonreducing conditions. The positions of reduced 330-kDa Tg at the end of the DTT treatment (*330 Red.*) and upon oxidation after DTT washout (*330-Ox.*) and of the intermolecular disulfide-linked adducts A, B, and C are indicated. *C*, PC Cl3 cells were pulse-labeled with ^{35}S-labeled amino acids in the presence of 0.2 mM DTT, washed, and chased for the indicated times. Cell lysates were immunoprecipitated with anti-Tg antibodies. Immunoprecipitates were resolved by SDS-PAGE under nonreducing conditions. The positions of the 330-kDa Tg and of the intermolecular disulfide-linked adducts (A, B, and C) are indicated.

Briefly, labeled cells were rinsed with PBS and then incubated for 30 min with 2 mM dithiobis(succinimidylpropionate) (DSP) freshly prepared in 90% PBS, 10% dimethyl sulfoxide. Cells were then rinsed with cold PBS and alkylated with 20 mM NEM. Cells were lysed with 1 ml of lysis buffer plus 20 mM NEM and 50 mM glycine to quench excess cross-linker. Lysates were then processed as described above.

For sequential immunoprecipitation, the samples were first immunoprecipitated under nondenaturing conditions and then brought to 5% SDS and boiled for 5 min. The samples were then diluted 10-fold with 1% Triton X-100, 150 mM NaCl, 25 mM Tris (pH 7.4) and reimmunoprecipitated. For three-step sequential immunoprecipitation, after the second step, samples were brought to 5% SDS and boiled for 5 min. The samples were again diluted 10-fold with 1% Triton X-100, 150 mM NaCl, 25 mM Tris (pH 7.4) and reimmunoprecipitated. Quantitation of labeled bands was performed using a PhosphorImager from Molecular Dynamics.

Co-immunoprecipitation of Defined Tg Regions with ER Oxidoreductases—293T were transiently transfected using Lipofectamine 2000 (Invitrogen) following the manufacturer's instructions. After 42 h of transfection, cells were treated with brefeldin A (5 μg/ml) for 6 h and then cross-linked *in situ* with 2 mM DSP as above. Cells were then washed in PBS containing 20 mM NEM and lysed as described above. Lysates were precleared with protein A-agarose, immunoprecipitated with anti-Tg, washed twice, and analyzed by reducing SDS-PAGE and immunoblotting.

RESULTS

Intermolecular Disulfide-linked Adducts of Tg Reflect Immature Conformations Distinguished by the State of Substrate Oxidation—Newly synthesized Tg can be resolved as multiple species upon nonreducing SDS-PAGE, including Tg monomers (330 kDa) and small amounts of higher molecular mass species termed adduct A (slowest migrating), adduct B, (intermediate mobility), and adduct C (fastest migrating), that appear transiently in pulse-chase experiments. The transient nature of these adducts is unaffected by treatment with proteasome inhibitors, suggesting that they are not primarily misfolded forms destined for endoplasmic reticulum-associated degradation but rather intermolecular adducts captured in the process of Tg intramolecular disulfide maturation (30). These adducts are fully dissociated under reducing conditions, and subcomponents of adduct B have been shown to contain Tg-ERp57 and Tg-PDI complexes (30).

To study initial disulfide-linked adduct formation, we analyzed the folding of Tg in a pulse-chase protocol in which initial oxidation in cultured thyrocytes (PC Cl3 cells) was inhibited during translation by the presence of various concentrations of dithiothreitol (DTT), followed by DTT washout. Upon metabolic labeling in the presence of either 0.5 or 0.75 mM DTT, no fully oxidized Tg could be recovered at the zero chase time but slowly appeared at 30 and 60 min of chase (Fig. 1*A*). However, washout of 0.5 or 0.75 mM DTT promoted Tg aggregation (bands entrapped in the stacking gel or just barely entering the running gel), which did not fully resolve even at 1 h of chase (Fig. 1*A*). Moreover, upon DTT washout, adduct species A and B appeared but with little or no formation of adduct C. Clearly, Tg folding was seriously perturbed by translation in these presence of these doses of DTT. By contrast, washout of a lower concentration of DTT (0.3 mM) allowed post-translational Tg oxidation to proceed near-normally: without disulfide-linked protein aggregates, with recovery of typical Tg adducts A, B, and C and with an increase in the overall recovery of labeled Tg (Fig. 1*A*). Indeed, low-dose DTT looked similar to chase samples that were pulse-labeled without DTT except that all Tg

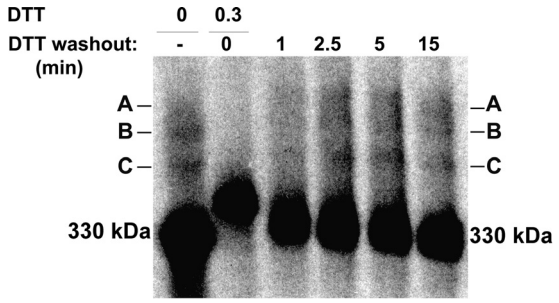

FIGURE 2. **Intermolecular disulfide-linked Tg adducts are not linked by a precursor-product relationship.** PC Cl3 cells were simultaneously treated with 0.3 mM DTT or not treated during pulse-labeling as described under "Experimental Procedures" and then washed and chased for the indicated times. *A*, cell lysates were immunoprecipitated with anti-Tg antibodies. Immunoprecipitates were resolved by SDS-PAGE under nonreducing conditions.

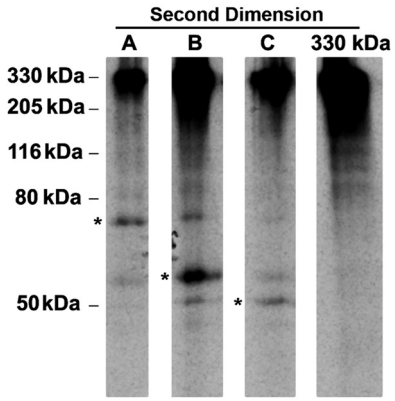

FIGURE 3. **Excision of adduct bands A, B, and C and second-dimensional SDS-PAGE analysis under reducing conditions.** PC Cl3 cells were metabolically labeled continuously for 48 h. Immunoprecipitated Tg was analyzed by nonreducing SDS-PAGE. The radioactive sample was exposed to film and realigned with the original sample, and disulfide-linked adducts A, B, and C and the original 330-kDa Tg band were selectively excised, eluted, and reanalyzed by SDS-PAGE under reducing conditions. Associated bands liberated upon reduction of Tg adducts are highlighted with *asterisks*; the positions of molecular mass markers (in kDa) are shown on the *left*.

adducts formed post-translationally (Fig. 1*B*). Thus, low-dose DTT, which blocked initial formation of Tg disulfide bonds, also blocked initial production of Tg adducts, and the appearance of adducts upon DTT washout correlated with intramolecular oxidative folding of Tg monomers (Fig. 1*B*).

Still lower concentrations of DTT (0.2 mM) allowed for the co-translational formation of Tg adducts (Fig. 1*C*). Interestingly, during the first 5 min after DTT washout from these conditions, the position of species A on the nonreducing gel notably shifted (Fig. 1*C*); bands B and C also showed small increases in their mobilities between 2.5 and 5 min of chase (Fig. 1*C*). We looked for evidence of a precursor-product relationships between the adduct species. After pulse-labeling in the presence of 0.3 mM DTT to reduce Tg, followed by short chase times to track the earliest post-translational formation of adducts, we observed initial oxidation of the 330-kDa Tg band within 1 min after DTT washout as disulfide-linked adducts A, B, and C first appeared (Fig. 2). Importantly, beginning at 2.5 min of chase, in parallel with oxidation of the 330-kDa Tg monomer band, each of the Tg adducts also showed an increase in their mobility (Fig. 2). A shift in mobility of adducts A, B, and C persisted even after removal of all *N*-linked glycans with PNGase F (data not shown). The data in Fig. 2 do not support a strict precursor-product relationship between adducts A, B, and C but suggest progression in the early oxidation of Tg within each of the adducts.

Defining the Molecular Components of Adducts A and C—We incubated PC Cl3 cells with ^{35}S-labeled amino acids for 48 h to label slow turnover ER resident proteins and immunoprecipitated Tg. To capture disulfide-linked Tg adducts, we ran a first-dimensional gel under nonreducing conditions and excised the individual adduct bands from the gel. Each band was then reanalyzed in a second dimensional gel under reducing conditions. Of course, each adduct regenerated a reduced 330-kDa Tg monomer under reducing conditions (the first-dimensional 330-kDa Tg oxidized band also regenerated a reduced 330-kDa reduced band, Fig. 3, *last lane*). In addition, each adduct preferentially released formerly disulfide-associated bands of molecular mass ~ 75, 59, and 50 kDa (*asterisk*, Fig. 3). As noted above, these bands are candidate ER oxidoreductases bound via transient mixed disulfide bonds to newly synthesized Tg. Indeed, we have already demonstrated that species B has two subcomponents containing oxidoreductases ERp57 and PDI (30).

We noted that in adduct A, a minor amount of 59 kDa and a very minor amount of 50 kDa bands accompanies the more abundant 75-kDa Tg-associated band. Similarly, in adduct B, moderate quantities of 75- and 50-kDa bands accompany the more abundant 59-kDa Tg-associated band. Finally, in adduct C, a minor amount of 59 kDa and an even minor amount of 75-kDa bands accompanies the more major 50-kDa Tg-associated band (Fig. 3). These potential co-complexes are considered further below.

On the basis of the molecular masses of the Tg-associated bands, we investigated whether the ~75-kDa band might represent ERp72 and whether the ~50-kDa band could represent CaBP1, the rat homolog of human P5. For this, we first immunoprecipitated with anti-ERp72 from cells that had been lysed and then incubated in either a denaturing or nondenaturing buffer, followed by SDS-PAGE analysis under nonreducing or reducing conditions. Anti-ERp72 immunoprecipitated a band co-migrating with disulfide-linked Tg adduct A, both under nondenaturing conditions (Fig. 4*A*, *lane 3*) and even after protein denaturation (*lane 4*). To confirm that this band A is indeed a disulfide-linked Tg-ERp72 adduct, we performed sequential IP in which Tg immunoprecipitates were denatured before a second round of immunoprecipitation with either anti-Tg or anti-ERp72. The result shown in Fig. 4*A*, *lane 8*, established that adduct A specifically contains both Tg and ERp72. Under reducing conditions, the Tg-ERp72 mixed disulfide bond was broken, and Tg contained within adduct A now ran as the 330-kDa monomer (Fig. 4*A*, *lanes 11*, *12*, and *16*).

Next, using denatured cell lysates, we performed immunoprecipitations with anti-CNX, anti-PDI, or anti-CaBP1/P5. Anti-CNX antibodies did not immunoprecipitate Tg adducts, confirming that CNX is not directly involved in mixed disulfides with Tg (Fig. 4*B*, *lane 2*). Anti-PDI immunoprecipitated the fast subcomponent of adduct B (Fig. 4*B*, *lane 3*), consistent with previous reports (30). And, strikingly, anti-CaBP1 anti-

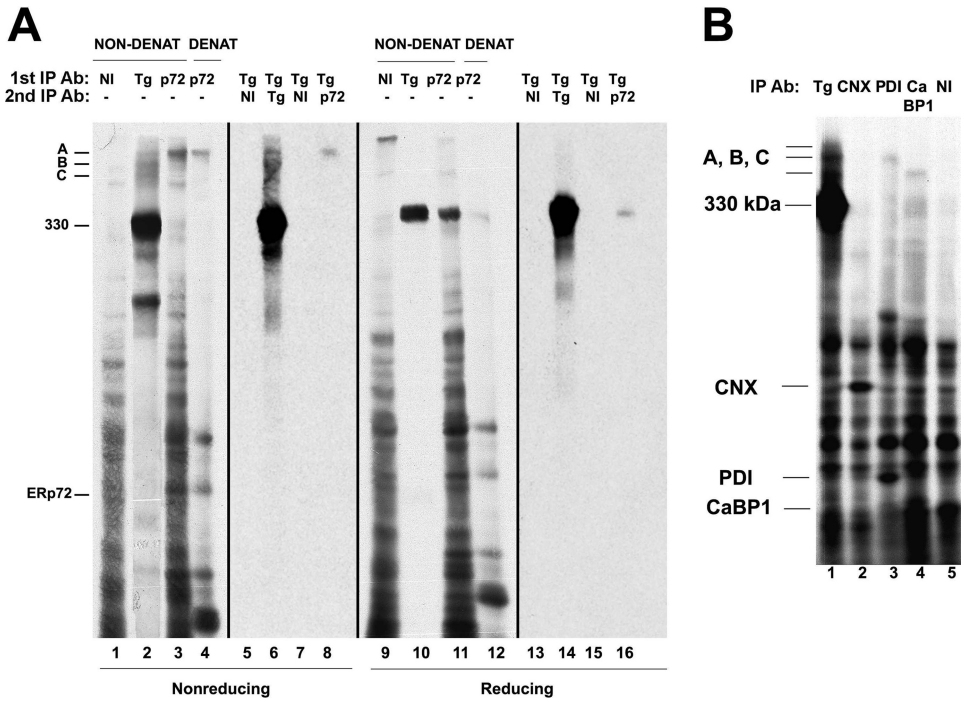

FIGURE 4. **Molecular composition of adduct A and C.** *A*, PC Cl3 cells were pulse-labeled as described under "Experimental Procedures" and lysed without chase. The cells were lysed under nondenaturing (*NON-DENAT*) or denaturing (*DENAT*) conditions, immunoprecipitated with nonimmune serum (*NI*), anti-Tg (sample overexposed), or anti-ERp72 (p72), and resolved by nonreducing (*lanes 1–4*) and reducing (*lanes 9–12*) SDS-PAGE. Alternatively, cell lysates were first immunoprecipitated with anti-Tg antibodies and then boiled in SDS, diluted into SDS-free immunoprecipitation buffer, and finally reimmunoprecipitated with nonimmune serum, anti-Tg, or anti-ERp72 antibodies (*Ab*). These re-precipitates were resolved by nonreducing (*lanes 5–8*) and reducing (*lanes 13–16*) SDS-PAGE. The 330-kDa molecular mass position and positions of intermolecular disulfide-linked Tg adducts A, B, and C and ERp72 are indicated. *B*, PC Cl3 cells were labeled and chased as described under "Experimental Procedures." Cell lysates were immunoprecipitated under denaturing conditions with nonimmune serum (*NI*), anti-Tg, anti-CNX, anti-PDI, and anti-CaBP1 antibodies and resolved by nonreducing SDS-PAGE. The positions of the 330-kDa Tg, intermolecular disulfide-linked Tg adducts (A, B, and C), CNX, PDI, and CaBP1 are indicated.

bodies immunoprecipitated adduct C (Fig. 4*B*, *lane 4*). Moreover, using siRNA-mediated knockdown of CaBP1/P5 expression (55–60% at the protein level) formation of adduct C was decreased, whereas steady-state levels of ERp72, ERp57, PDI, CNX, BiP, and CRT appeared unaffected (Fig. 5*A* gels at *left*). Accordingly, the ratios of adducts C:A or C:B decreased, whereas the A:B ratio did not change (Fig. 5*A*, *right*). Similarly, siRNA-mediated ERp72 knockdown (55% at the protein level) correlated with a decrease in adduct A (Fig. 5*B*).

We noted that upon exposure to lower doses of DTT during metabolic labeling, adduct A appeared most sensitive (*first lane* of Fig. 1*C*) yet following washout of higher doses of DTT, adduct A (and B) formed in preference to adduct C (Fig. 1*A*). As the mobility differences between adducts A and C appear too great to be accounted for solely by molecular mass differences between individual ER oxidoreductases, these results seem to signify that in the complex primarily bearing ERp72, Tg may be in a very open, easily reduced conformation, whereas in the complex primarily bearing CaBP1/P5, a somewhat different pattern of disulfide bonds within the component Tg monomers may prevail.

A Tg-ERp57 mixed disulfide interaction has been found within a subcomponent of Tg adduct B, which is dependent on a lectin-like CRT/CNX interaction with Tg that is abrogated by pretreatment of thyrocytes with castanospermine that inhibits ER glucosidases I and II (22, 30). As expected, when cells were pretreated with 0.1 mg/ml castanospermine before metabolic labeling, formation of CaBP1/P5-containing Tg adducts was unaffected, and ERp72-containing Tg adducts were actually increased (data not shown). Thus, similar to other glycoprotein substrates (18, 19), Tg forms ERp72- and CaBP1/P5-containing mixed disulfide complexes independently from its interactions with lectins CRT/CNX.

Regional Binding of ER Oxidoreductases along the Tg Molecule—The Tg monomer is a protein of ~2750 residues containing 122 cysteine residues that could serve as potential sites of mixed disulfide bond formation. As noted under the Introduction, Tg structure is subdivided into Region I (bearing type 1 repeats), II–III (bearing types 2 and 3 repeats), and C-terminal ChEL domains. We examined regional association of ER oxidoreductases with Tg constructs encoding I-II-II, secretory II-III, and secretory ChEL (with each protein containing a signal peptide for delivery into the secretory pathway and C-terminally tagged with an HA epitope (34, 23)). Transfected 293T cells were treated with brefeldin A for 6 h to ensure ER accumulation of each construct. Nearest neighbor cell proteins were cross-linked with DSP, and the cells were lysed, immunoprecipitated with anti-Tg, and analyzed by SDS-PAGE and Western blotting with selected antibodies. The Tg construct recovered most abundantly from cells was II-III-HA and the least abundant was ChEL-HA (Fig. 6*A*). When comparing ER oxidoreductase associations with these two constructs, it was clear that pulldown of II-III co-precipitated more ERp72 and CaBP1 than did ChEL (Fig. 6, *B* and *C*), whereas pulldown of ChEL co-precipitated more PDI than did II-III (Fig. 6*D*), and co-precipitation of ERp57 appeared comparable (Fig. 6*E*). Although

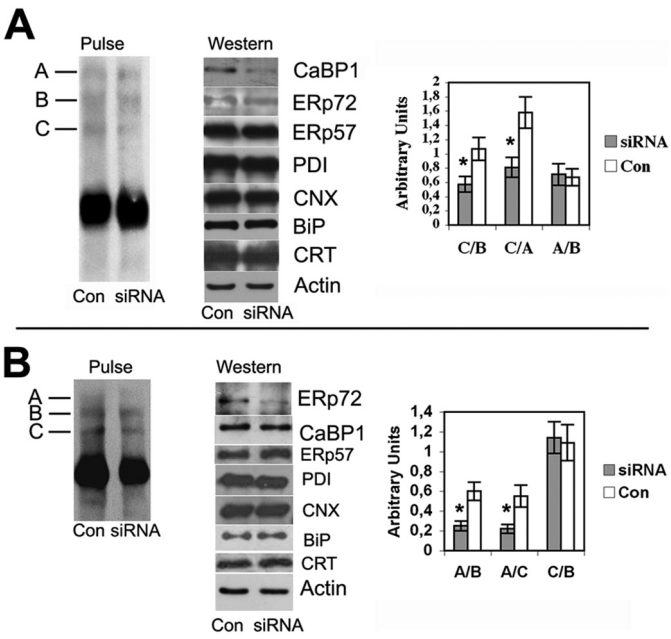

FIGURE 5. **Levels of ERp72 and CaBP1 are linked to the formation of Tg adducts A and C, respectively.** CaBP1/P5 levels (*A*) or ERp72 levels (*B*) were decreased in PC Cl3 cells by specific siRNA-mediated knockdown, as described under "Experimental Procedures." Equivalent amounts of cell lysates were immunoblotted for PDI family members, ER chaperones, and actin. In the same experiment, cells were pulse-labeled with ^{35}S-labeled amino acids, and cell lysates were immunoprecipitated with anti-Tg antibodies and analyzed by SDS-PAGE under nonreducing conditions (*left panels*). The positions of the intermolecular disulfide-linked adducts (A, B, and C) are indicated. *Panels at right*: The various adduct ratios were calculated from five independent knockdown experiments. *, $p < 0.05$. *Con*, control.

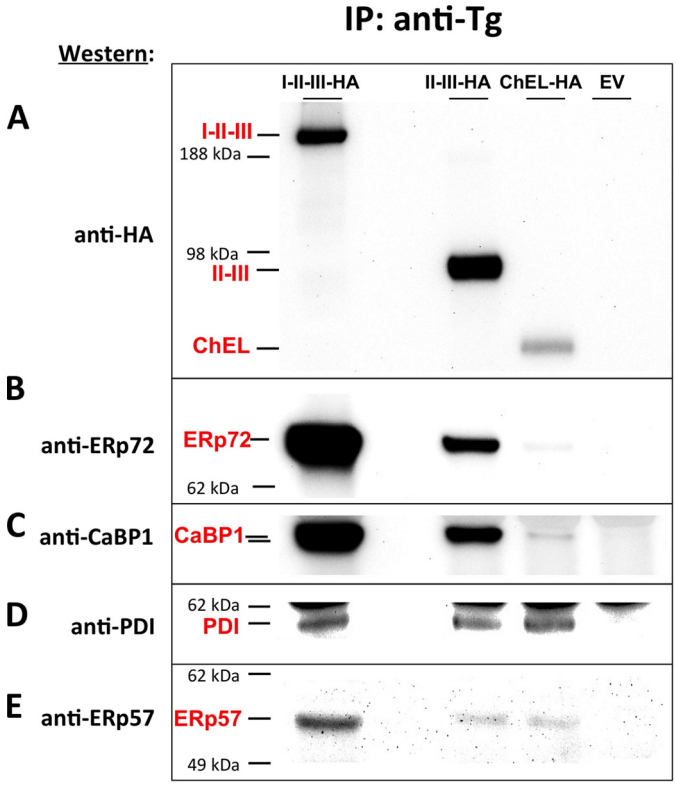

FIGURE 6. **Tg regional interactions with ERp72, CaBP1, PDI and ERp57.** 293T cells were transfected to express the constructs indicated; each construct was C-terminally tagged with a single HA epitope. Empty vector (*EV*) was used as a negative control. Following treatment with brefeldin A (5 μg/ml, 6 h), cells were cross-linked with DSP (2 mM, in PBS for 30 min at room temperature), lysed, and immunoprecipitated with anti-Tg antibodies. The immunoprecipitates were resolved by SDS-PAGE and electrotransfer to nitrocellulose and analyzed by Western blotting with anti-HA (*A*), anti-ERp72 (*B*), anti-CaBP1 (*C*), anti-PDI (*D*), or anti-ERp57 (*E*) antibodies. Representative results of four independent experiments are shown. The positions of the Tg regions I-II-III, II-III, ChEL, and ERp72, CaBP1, PDI, and ERp57 and selected molecular weight standards are indicated.

the data indicate an oxidoreductase preference of ChEL for association with PDI and II-III for association with ERp72 and CaBP1, it was clear in every instance that the combined regions I-III-III co-precipitated more of each oxidoreductase than other constructs. These data suggest by inference that region I, bearing the majority of Tg cysteine residues (28), may be a major interaction region for ERp72 and CaBP1 and associated molecular chaperones, and this was confirmed in independent cross-linking and co-precipitation experiments (data not shown) (23). Indeed, results obtained after metabolic pulse-labeling with ^{35}S-labeled amino acids in cells untreated with brefeldin A (data not shown) also were consistent with preferential binding of ER oxidoreductases to region I. Taken together, these data suggest that regions I, II-III, and ChEL each interact with all of the tested ER oxidoreductases but to a different extent.

The same Tg Molecule Can Form Simultaneous Mixed Disulfides with PDI and CaBP1/P5—Recently, CaBP1/P5, and to a lesser extent ERp72, have been shown to exist in specific chaperone complexes with BiP and GRP94, whereas PDI was not found associated with these chaperones (18). These results raise the possibility that substrate specificity of these oxidoreductases, similar to that for ERp57 (14, 19), may be facilitated by additional noncovalent interactions with specific ER chaperones. Given the known interaction of Tg with multiple chaperones (22, 29) and association of ER oxidoreductases with distinct regions along the Tg molecule (Fig. 6), it was reasonable to examine the possibility of multiple simultaneous oxidoreductase partners with full-length Tg. For this, immunoprecipitates of newly synthesized Tg were reimmunoprecipitated sequentially either with anti-PDI followed by anti-CaBP1, or reciprocally reimmunoprecipitated with anti-CaBP1 followed by anti-PDI. Strikingly, anti-CaBP1 antibodies were able to reimmunoprecipitate some of the Tg contained in PDI immunoprecipitates (Fig. 7, *lane 9*). Similarly, anti-PDI antibodies immunoprecipitated some of the Tg contained in CaBP1 immunoprecipitates (*lane 7*). Thus, adduct C (that is enriched in CaBP1/P5, Fig. 3) also contains some PDI molecules (Fig. 7, *lane 9*), whereas adduct B that is enriched in PDI also contains some CaBP1 molecules (Fig. 7, *lane 7*). These results indicate that PDI and CaBP1/P5 can simultaneously engage the same Tg molecule, most likely at different places along the length of the Tg polypeptide.

This finding supports the possibility that Tg molecules are also simultaneously engaged with distinct noncovalently associated ER molecular chaperones that help recruit their ER oxidoreductase partners to their preferred sites of action. To examine this, PC Cl3 cells were metabolically labeled to steady state and cross-linked before cell lysis. Tg immunoprecipitates from the cell lysates were then either reimmunoprecipitated with anti-Tg or with antibodies against ER chaperones (Fig. 8,

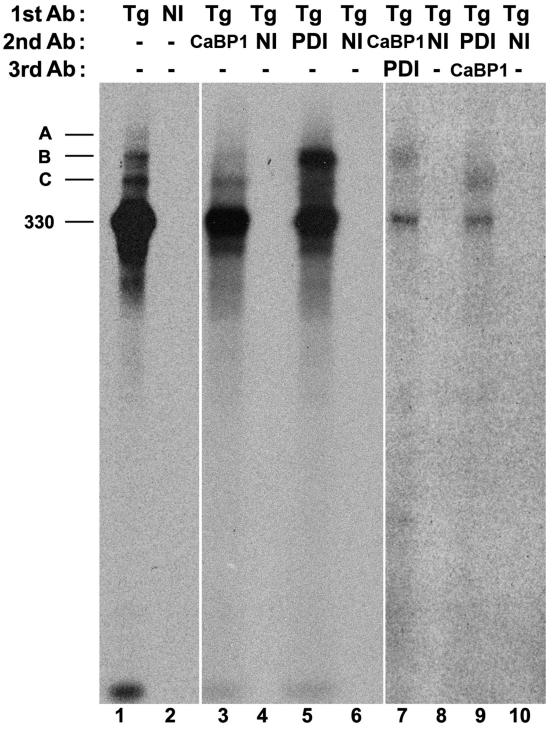

FIGURE 7. **Both PDI and CaBP1 form mixed disulfides with the same Tg molecules.** PC Cl3 cells were pulse-labeled and chased for 15 min as described under "Experimental Procedures." Cell lysates were first immunoprecipitated with anti-Tg antibodies, boiled in SDS, and reimmunoprecipitated with nonimmune serum (*NI*) or anti-PDI or anti-CaBP1 antibodies (*Ab*). The second immunoprecipitate was boiled in SDS and reciprocally immunoprecipitated (the anti-PDI second immunoprecipitate reimmunoprecipitated with anti-CaBP1 and the anti-CaBP1 immunoprecipitate reimmunoprecipitated with anti-PDI) and the samples resolved by nonreducing SDS-PAGE. The 330-kDa molecular mass position, and the positions of intermolecular disulfide-linked Tg adducts A, B, and C are indicated. *Lanes 1* and *2* were exposed 1 day; *lanes 3–6* were exposed 3 days; *lanes 7–10* were exposed 20 days.

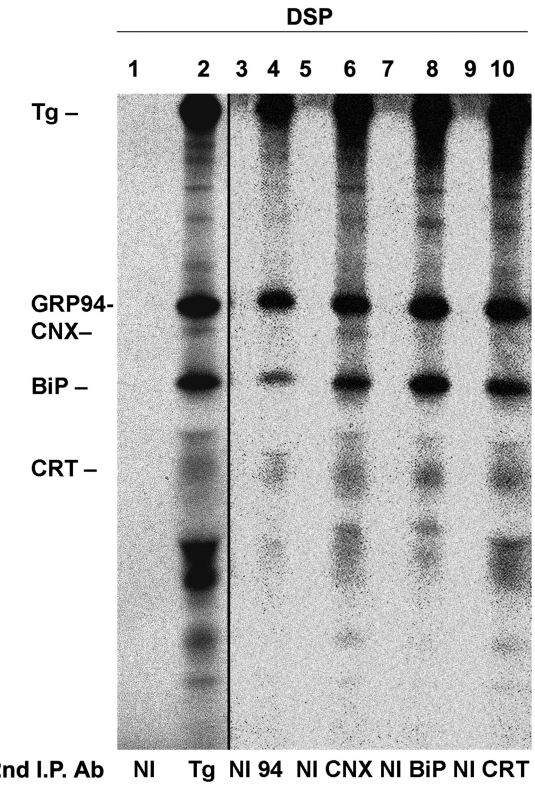

FIGURE 8. **Intracellular Tg associates with multiple ER chaperones.** PC Cl3 cells were metabolically labeled continuously for 48 h. Intact cells were cross-linked with a membrane-permeant, thiol-cleavable cross-linker DSP. Cell lysates were immunoprecipitated first with anti-Tg antibodies (*Ab*) and then reimmunoprecipitated either with anti-Tg (*lane 2*), anti-GRP94 (*lane 4*), anti-CNX (*lane 6*), anti-BiP (*lane 8*), anti-CRT (*lane 10*), or non-immune serum (*NI*). The positions of the 330-kDa Tg, GRP94, BiP, CNX, and CRT are indicated. The anti-Tg immunoprecipitates were exposed 1 day, and the anti-chaperone immunoprecipitates were exposed 5 days.

lanes 1–10). Anti-Tg antibodies co-precipitated a series of bands highly reminiscent of those reported to associate with ER-misfolded IgG heavy chain (17). Immunoprecipitation of CRT or CNX, which are known to associate with the ERp57 oxidoreductase, immunoprecipitated the same pattern of bands. These data are consistent with the idea that a subset of Tg molecules can associate simultaneously with CRT/CNX (and associated ERp57) as well as BiP/GRP94 (and associated CaBP1/P5 (18)).

DISCUSSION

ER members of the PDI superfamily may have overlapping/interchangeable activities, or may be dedicated to distinct enzyme-catalyzed reactions or distinct substrates (4–7, 35, 36). Secretory proteins such as Tg (which make ~60 intrachain disulfide bonds) are potential substrates for multiple ER oxidoreductases that participate in oxidative protein folding. Given the extensive intradomain disulfide bonding within Tg (22, 28), the participation of multiple ER oxidoreductases in Tg folding should be anticipated.

We hypothesize that the detection of disulfide-linked Tg adducts captures mixed disulfide complexes occurring at a moment in the catalytic cycle of a variety of oxidoreductases in the ER. What is known is that Tg strongly interacts with lectin-like chaperones, especially CRT (22) to facilitate association with the ERp57 oxidoreductase, and Tg-PDI association has also been demonstrated, comprising two subcomponents of adduct B (30). Tg adducts appear when Tg oxidative folding appears (Fig. 2); thus, these adducts are of extreme interest as candidate folding intermediates for Tg. Herein, we have sought to determine the identity of Tg adducts A and C and found that adduct A is enriched in ERp72 and adduct C is enriched in CaBP1, the equivalent of the human P5. Interestingly, reanalysis of each adduct band by reducing SDS-PAGE yields Tg molecules not only with the primary-associated ER oxidoreductase but also with additional co-associated ER oxidoreductases. Furthermore, a three-step sequential immunoprecipitation establishes that there are some CaBP1/P5 molecules covalently bound to the Tg-PDI predominant adducts, and some PDI molecules covalently bound to the Tg-CaBP1/P5 predominant adducts (Fig. 7). This is consistent with binding sites for ER oxidoreductases in the multiple distinct regions of the Tg molecules (Fig. 6). Thus, we conclude that the same newly synthesized Tg molecule simultaneously engages more than one ER oxidoreductase, each working on its respective preferred binding site, in a kinetically overlapping way.

The specific Cys residues within the distinct regions of nascent Tg that bind to distinct oxidoreductases remain unknown. However, within the last decade, the concept of different "chaperone systems" has come into favor (17). In this

view, PDI does not primarily work together with BiP (19), whereas ERp72 and CaBP1 may do so preferentially (18). In such a model, the substrate specificity of distinct ER oxidoreductases may be driven by their association(s) with a given chaperone or set of chaperones (13, 14, 18, 37). Thus far, simultaneous interactions with multiple ER chaperones and oxidoreductases has been reported mostly for misfolded mutant proteins, including Tg (38), in which some oxidoreductase interactions may promote endoplasmic reticulum-associated degradation of the substrate (39). However, even for wild-type Tg, dissociation from CRT/CNX occurs with kinetics that overlap with the dissociation of Tg from BiP/GRP94 (22, 29, 40). Indeed, under physiological conditions, it is impossible to observe completely sequential handling of Tg by different chaperones (30), and this supported in the current study (Fig. 8). If these distinct chaperone interactions help to present domains of the Tg substrate to the appropriate oxidoreductases, then these oxidoreductases may be bound simultaneously to Tg as well. The large Tg polypeptide with its distinct folding domains can certainly accomodate activities of multiple simultaneous ER chaperone-oxidoreductase complexes acting along the length of the Tg molecule. Presumably, it is this very feature that increases the efficiency in catching Tg in transient mixed disulfide adducts.

Our data are also consistent with the idea described above that distinct adducts may capture Tg during the progression of oxidative maturation in distinct regions. Interestingly, oxidative maturation appears to continue, seemingly within the adducts, in parallel with the oxidative maturation of Tg monomers (Fig. 2). As the time needed to complete one catalytic cycle for each ER oxidoreductase is believed to be quite short, the likelihood is that each newly synthesized Tg molecule is in essence shuttling progressively between covalent adduct and "monomeric" folding intermediate that represents the noncovalent association with chaperone-oxidoreductase complexes. (Thus, the labeled Tg molecules present in the ERp72-enriched adduct A at 15 min after synthesis may well be different Tg molecules than the ones present in adduct A at 2.5 min.)

A priori, one might have expected that as oxidation proceeds, Tg molecules would successively form adduct A, B, and C. However, as best as can be discerned, adducts A, B, and C do not follow a precursor-product relationship. Rather, we hypothesize that when one kind of chaperone-oxidoreductase complex is predominantly associated, this leads to the formation of a particular adduct band, with lower levels of secondarily bound oxidoreductases on other parts of the Tg molecule. Predominance of a different chaperone/oxidoreductase association may trigger preferred initial oxidative folding in a different Tg region, while secondarily permitting other chaperone/oxidoreductase partners to associate. Ultimately, all parts of the Tg molecule achieve oxidative maturity and at such times, adducts disappear. If this is correct, then one may hypothesize parallel tracks of early oxidative folding of wild-type Tg leading to the native, transport-competent state. Precisely such a role for chaperone/oxidoreductase assistance fits with a model of local protein structural optimization during global conformational maturation (41).

In conclusion, we believe that we have now identified the major ER oxidoreductases involved in early Tg oxidative folding. These ER oxidoreductases may facilitate multiple parallel pathways of local Tg maturation, captured in transient distinct mixed-disulfide adducts, with simultaneous engagement of distinct chaperone-oxidoreductase complexes associated with Tg in different ratios.

REFERENCES

1. Rutkevich, L. A., and Williams, D. B. (2011) Participation of lectin chaperones and thiol oxidoreductases in protein folding within the endoplasmic reticulum. *Curr. Opin. Cell. Biol.* **23,** 157–166
2. Braakman, I., and Bulleid, N. J. (2011) Protein folding and modification in the mammalian endoplasmic reticulum. *Annu. Rev. Biochem.* **80,** 71–99
3. Sevier, C. S., and Kaiser, C. A. (2002) Formation and transfer of disulphide bonds in living cells. *Nat. Rev. Mol. Cell Biol.* **3,** 836–847
4. Ellgaard, L., and Ruddock, L. W. (2005) The human protein disulphide isomerase family: substrate interactions and functional properties. *EMBO Rep.* **6,** 28–32
5. Hatahet, F., and Ruddock, L. W. (2007) Substrate recognition by the protein disulfide isomerases. *FEBS J.* **274,** 5223–5234
6. Margittai, E., and Sitia, R. (2011) Oxidative protein folding in the secretory pathway and redox signaling across compartments and cells. *Traffic* **12,** 1–8
7. Kakihana, T., Nagata, K., and Sitia, R. (2012) Peroxides and peroxidases in the endoplasmic reticulum: integrating redox homeostasis and oxidative folding. *Antioxid. Redox. Signal.* **16,** 763–771
8. Lyles, M. M., Gilbert, H. F. (1991) Catalysis of the oxidative folding of ribonuclease A by protein disulfide isomerase: pre-steady-state kinetics and the utilization of the oxidizing equivalents of the isomerase. *Biochemistry* **30,** 619–625
9. Bulleid, N. J., and Freedman, R. B. (1988) Defective co-translational formation of disulphide bonds in protein disulphide-isomerase-deficient microsomes. *Nature* **335,** 649–651
10. Kulp, M. S., Frickel, E. M., Ellgaard, L., and Weissman, J. S. (2006) Domain architecture of protein-disulfide isomerase facilitates its dual role as an oxidase and an isomerase in Ero1p-mediated disulfide formation. *J. Biol. Chem.* **281,** 876–884
11. Oliver, J. D., Roderick, H. L., Llewellyn, D. H., and High, S. (1999) ERp57 functions as a subunit of specific complexes formed with the ER lectins calreticulin and calnexin. *Mol. Biol. Cell* **10,** 2573–2582
12. Maattanen, P., Kozlov, G., Gehring, K., Thomas, D. Y. (2006) ERp57 and PDI: multifunctional protein disulfide isomerases with similar domain architectures but differing substrate-partner associations. *Biochem. Cell Biol.* **84,** 881–889
13. Zapun, A., Darby, N. J., Tessier, D. C., Michalak, M., Bergeron, J. J., and Thomas, D. Y. (1998) Enhanced catalysis of ribonuclease B folding by the interaction of calnexin or calreticulin with ERp57. *J. Biol. Chem.* **273,** 6009–6012
14. Jessop, C. E., Tavender, T. J., Watkins, R. H., Chambers, J. E., and Bulleid, N. J. (2009a) Substrate specificity of the oxidoreductase ERp57 is determined primarily by its interaction with calnexin and calreticulin. *J. Biol. Chem.* **284,** 2194–2202
15. Schelhaas, M., Malmström, J., Pelkmans, L., Haugstetter, J., Ellgaard, L., Grünewald, K., and Helenius, A. (2007) Simian Virus 40 depends on ER protein folding and quality control factors for entry into host cells. *Cell* **131,** 516–529
16. Zhang, Y., Kozlov, G., Pocanschi, C. L., Brockmeier, U., Ireland, B. S., Maattanen, P., Howe, C., Elliott, T., Gehring, K., and Williams, D. B. (2009) ERp57 does not require interactions with calnexin and calreticulin to promote assembly of class I histocompatibility molecules, and it enhances peptide loading independently of its redox activity. *J. Biol. Chem.* **284,** 10160–10173
17. Meunier, L., Usherwood, Y. K., Chung, K. T., and Hendershot, L. M. (2002) A subset of chaperones and folding enzymes form multiprotein complexes in endoplasmic reticulum to bind nascent proteins. *Mol. Biol. Cell* **13,** 4456–4469

18. Jessop, C. E., Watkins, R. H., Simmons, J. J., Tasab, M., and Bulleid, N. J. (2009b) Protein disulphide isomerase family members show distinct substrate specificity: P5 is targeted to BiP client proteins. *J. Cell Sci.* **122,** 4287–4295
19. Soldà, T., Garbi, N., Hämmerling, G. J., and Molinari, M. (2006) Consequences of ERp57 deletion on oxidative folding of obligate and facultative clients of the calnexin cycle. *J. Biol. Chem.* **281,** 6219–6226
20. Kim, P. S., and Arvan, P. (1991) Folding and assembly of newly synthesized thyroglobulin occurs in a pre-Golgi compartment. *J. Biol. Chem.* **266,** 12412–12418
21. Di Jeso, B., and Arvan, P. (2004). Thyroglobulin Structure, Function, and Biosynthesis in *The Thyroid* (Braverman, L. E., and Utiger, R., eds) 9th Ed., pp. 77–95, Lippincott Williams & Wilkins, Philadelphia, PA
22. Di Jeso, B., Ulianich, L., Pacifico, F., Leonardi, A., Vito, P., Consiglio, E., Formisano, S., and Arvan, P. (2003) The folding of thyroglobulin in the calnexin/ calreticulin pathway and its alteration by a loss of Ca2 from the endoplasmic reticulum. *Biochem. J.* **370,** 449–458
23. Lee, J., and Arvan, P. (2011) Repeat motif-containing regions within thyroglobulin. *J. Biol. Chem.* **286,** 26327–26333
24. Neumann, G. M., and Bach, L. A. (1999) The N-terminal disulfide linkages of human insulin-like growth factor-binding protein-6 (hIGFBP-6) and hIGFBP-1 are different as determined by mass spectrometry. *J. Biol. Chem.* **274,** 14587–14594
25. Chong, J. M., and Speicher, D. W. (2001) Determination of disulfide bond assignments and *N*-glycosylation sites of the human gastrointestinal carcinoma antigen GA733–2 (CO17–1A, EGP, KS1–4, KSA, and Ep-CAM). *J. Biol. Chem.* **276,** 5804–5813
26. Lee, J., Di Jeso, B., and Arvan, P. (2008) The cholinesterase-like domain of thyroglobulin functions as an intramolecular chaperone. *J. Clin. Invest.* **118,** 2950–2958
27. Wang, X., Lee, J., Di Jeso, B., Treglia, A. S., Comoletti, D., Dubi, N., Taylor, P., and Arvan, P. (2010) Cis and trans actions of the cholinesterase-like within the thyroglobulin dimer. *J. Biol. Chem.* **285,** 17564–17573
28. Lee, J., Di Jeso, B., and Arvan P. (2011) Maturation of thyroglobulin protein region I. *J. Biol. Chem.* **286,** 33045–33052
29. Kim, P. S., and Arvan, P. (1995) Calnexin and BiP act as sequential molecular chaperones during thyroglobulin folding in the endoplasmic reticulum. *J. Cell Biol.* **128,** 29–38
30. Di Jeso, B., Park, Y. N., Ulianich, L., Treglia, A. S., Urbanas, M. L., High, S., and Arvan, P. (2005) Mixed-disulfide folding intermediates between thyroglobulin and endoplasmic reticulum resident oxidoreductases ERp57 and protein disulfide isomerase. *Mol. Cell Biol.* **25,** 9793–9805
31. Di Jeso, B., Liguoro, D., Ferranti, P., Marinaccio, M., Acquaviva, R., Formisano, S., and Consiglio, E. (1992) Modulation of the carbohydrate moiety of thyroglobulin by thyrotropin and calcium in Fisher rat thyroid line-5 cells. *J. Biol. Chem.* **267,** 1938–1944
32. Ulianich, L., Garbi, C., Treglia, A. S., Punzi, D., Miele, C., Raciti, G. A., Beguinot, F., Consiglio, E., and Di Jeso, B. (2008) ER stress is associated with dedifferentiation and an epithelial-to-mesenchymal transition-like phenotype in PC Cl3 thyroid cells. *J. Cell Sci.* **121,** 477–486
33. Muresan, Z., and Arvan, P. (1997) Thyroglobulin transport along the secretory pathway. Investigation of the role of molecular chaperone, GRP94, in protein export from the endoplasmic reticulum. *J. Biol. Chem.* **272,** 26095–26102
34. Lee, J., Wang, X., Di Jeso, B., and Arvan, P. (2009) The cholinesterase-like domain, essential in thyroglobulin trafficking for thyroid hormone synthesis, is required for protein dimerization. *J. Biol. Chem.* **284,** 12752–12761
35. Mezghrani, A., Fassio, A., Benham, A., Simmen, T., Braakman, I., and Sitia, R. (2001) Manipulation of oxidative protein folding and PDI redox state in mammalian cells. *EMBO J.* **20,** 6288–6296
36. Rutkevich, L. A., Cohen-Doyle, M. F., Brockmeier, U., and Williams, D. B. (2010) Functional relationship between protein disulfide isomerase family members during the oxidative folding of human secretory proteins. *Mol. Biol. Cell* **21,** 3093–3105
37. Jessop, C. E., Chakravarthi, S., Garbi, N., Hämmerling, G. J., Lovell, S., and Bulleid, N. J. (2007) ERp57 is essential for efficient folding of glycoproteins sharing common structural domains. *EMBO J.* **26,** 28–40
38. Menon, S., Lee, J., Abplanalp, W. A., Yoo, S. E., Agui, T., Furudate, S., Kim, P. S., Arvan, P. (2007) Oxidoreductase interactions include a role for ERp72 engagement with mutant thyroglobulin from the rdw/rdw rat dwarf. *J. Biol. Chem.* **282,** 6183–6191
39. Forster, M. L., Sivick, K., Park, Y. N., Arvan, P., Lencer, W. I., Tsai, B. (2006) Protein disulfide isomerase-like proteins play opposing roles during retrotranslocation. *J. Cell Biol.* **173,** 853–859
40. Kim, P. S., Bole, D., and Arvan, P. (1992) Transient aggregation of nascent thyroglobulin in the endoplasmic reticulum: relationship to the molecular chaperone, BiP. *J. Cell Biol.* **118,** 541–549
41. Dill, K. A., Ozkan, S. B., Shell, M. S., and Weikl, T. R. (2008) The protein folding problem. *Annu. Rev. Biophys.* **37,** 289–316